Group Art Unit: 2884
Examiner: Lee, S.

Atty. Ref.: H 2182

IN THE UNITED STATES PATENT AND TRADEMARK OFFICE

Applicants   :   Martin Klein et al.

Appl. No.   :   10/047,556

Filed   :   October 23, 2001

For   :   DETECTOR

MS Amendment
Commissioner for Patents
P.O. Box 1450
Alexandria, VA 22313-1450

RULE 132 DECLARATION

Sir:

I, Martin Klein, am a citizen of Germany and reside at Glauchauer Weg 10, 68309 Mannheim (new address) (old address: Seckenheimer Strasse 46 B, Mannheim 68165), Germany. I have a doctorate degree in Physics and I am currently employed by Heidelberg University.

I am one of the two named inventors in the above-captioned United States patent application and I am familiar with my patent application. I also studied and am familiar with U.S. Patent No. 6,429,578 which issued to Danielsson et al.

I conducted simulation analyses to compare absorption efficiencies of three different converter devices. It has been my experience that the simulation program I used provides a close approximation of actual tests. Additionally, the simulation analysis is very good for comparing the absorption efficiencies of different converter devices.

The Danielsson et al. patent focuses on the detection of X-rays. As a result, my simulation analyses were carried out to compare absorption efficiency for X-rays having energies between 10 keV and 150 keV.

The first converter device simulated in my analysis was a conventional GEM foil having copper electrodes with thicknesses of 5 micrometers disposed on opposite respective sides of an insulator. The absorption efficiencies for that simulation are represented by the lowermost line on the graph attached to this Declaration.

The second converter device that was subject to my simulation analysis had an additional layer of copper of 5 micrometer thickness on one of the copper electrodes of the conventional GEM foil used in the first analysis. As a result, the second simulation had a copper layer of 10 micrometers thick on one side of the insulator. This second simulation analysis was intended to simulate the embodiment of Danielesson et al. set forth in claim 11 of the Danielsson et al. patent. Absorption efficiencies for that second simulation are represented by the center line in the graph.

The third converter device simulated in my analysis had a 5 micrometer thick layer of gold on the copper electrode on one side of the conventional GEM foil. Thus, the third test sample conforms to the claims of my above-captioned patent application in that the converter layer is formed of a material different than the conductive layer on which the converter layer is arranged. My patent application focuses on neutron detection, and gold would not be chosen as a converter layer for neutron detection. Conversely, the converter layers used for neutron detection would not be used for X-ray detection. I chose a gold converter layer for the third simulation to provide a meaningful comparison to Danielsson
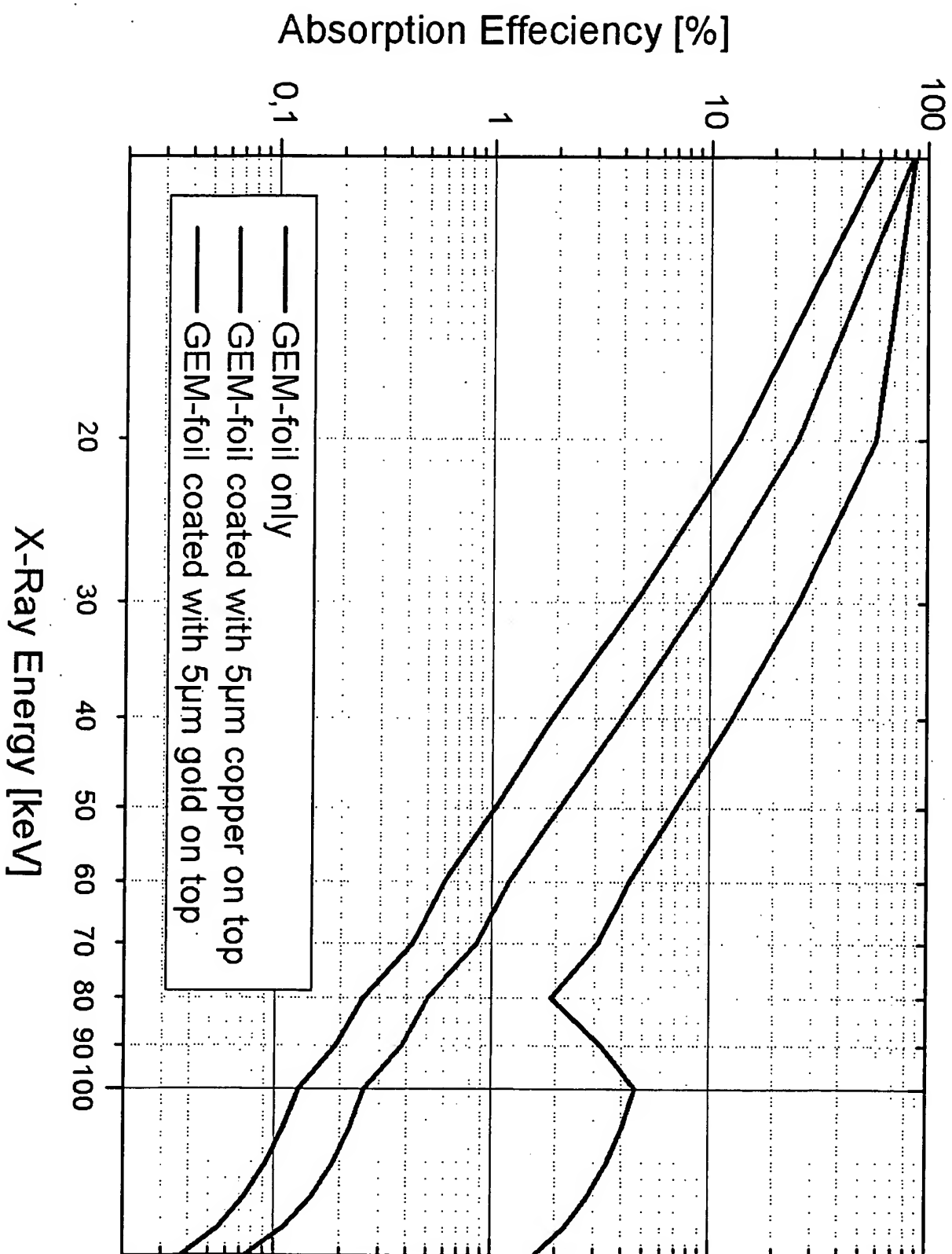
2

et al. The absorption efficiencies for the third simulation are shown by the uppermost line in the graph.

The vertical axis in the attached graph represents absorption efficiencies and is presented as a logarithmic scale. The attached graph shows very significantly enhanced absorption efficiencies for the third simulation (i.e., my claimed invention) as compared to either the first or second simulations. In particular, efficiencies achieved by the third simulation (the claimed invention herein) can be as much as ten times higher than the absorption efficiencies for the second simulation (Danielsson et al.). The magnitude of this enhanced absorption efficiency of the third simulation was greater than I would have expected.

I declare that all statements made herein on my own knowledge are true and that all statements made on information and belief are believed to be true and further that these statements are made with the knowledge that willful false statements and the like so made are punishable by fine or imprisonment, or both, under Section 1001 of Title 18 of the United States code and that such willful false statements will jeopardize the validity of this application and any patent issued thereon.

Dr. Martin Klein

Martin Klein

Date: _Heidelberg,_
_5. 5. 2006_

3

Absorption Effeciency [%]

100

10

1

0,1

GEM-foil only
GEM-foil coated with 5µm copper on top
GEM-foil coated with 5µm gold on top

20 30 40 50 60 70 80 90 100

X-Ray Energy [keV]

Advances in Gas Avalanche Photomultipliers[*]

A. Breskin[1], T. Boutboul, A. Buzulutskov[2], R. Chechik, G. Garty,
E. Shefer and B. K. Singh

Department of Particle Physics, The Weizmann Institute of Science
76100, Rehovot, Israel

Abstract

Gas avalanche detectors, combining solid photocathodes with fast electron multipliers, provide an attractive solution for photon localization over very large sensitive areas and under high illumination flux. They offer single photon sensitivity and the possibility of operation under very intense magnetic fields.

We discuss the principal factors governing the operation of gas avalanche photomultipliers. We summarize the recent progress made in alkali-halide and CVD-diamond UV-photocathodes, capable of operation under gas multiplication, and novel thin-film protected alkali-antimonide photocathodes, providing, for the first time, the possibility of operating gas photomultipliers in the visible range.

Electron multipliers, adequate for these photon detectors, are proposed and some applications are briefly discussed.

---

[*] Talk by A. Breskin, dedicated to the memory of the late Pierre Besson.
[1] Corresponding author, fnbresk@wisemail.weizmann.ac.il
[2] Present address: BINP, Novosibirsk, Russia

1. Introduction

In recent years there have been considerable advances in photon detectors, motivated by the ever-growing complexity of their potential applications. High-resolution localization of light, over a broad spectrum ranging from far UV to the IR, often down to a single-photon level, is requested in various basic and applied fields. Numerous examples can be found in particle and nuclear physics, astrophysics, medical imaging etc.

Present photon detection techniques range from tiny cryogenic detectors, employed in astrophysics, through a variety of small-area solid-state detectors, to vacuum-based devices - reaching dimensions of up to half a meter in diameter. The latter are photomultipliers developed for large under-water astro-particle experiments and are not position-sensitive. Commercially manufactured position sensitive vacuum photomultipliers are limited in size to a few inches in diameter, suffer from a degraded response in moderate magnetic fields and are rather expensive. Intensive research and development work is taking place in the more recently introduced hybrid photo detectors (HPD) [1]. These vacuum-operated devices could be, in principle, more immune to magnetic fields; 5 inch in diameter HPDs, with a highly pixelized readout, are being developed for particle identification by the Ring Imaging Cherenkov (RICH) technique, in the field of particle- and astro-particle physics [2].

In most experiments, the RICH technique requires the coverage of very large photon detection areas, typically of several square meters, good localization accuracy and high sensitivity to single Cherenkov photons. Numerous other applications, such as photon recording from large arrays of scintillators or scintillating fibers also require fast, large area, photon detectors, and often immune to magnetic fields.

Therefore, a large variety of gas-
3], have been developed over the last two decades and are successfully employed in numerous experiments. The first generation of such detectors consisted of wire chambers, filled with an UV- photosensitive gas (TEA, TMAE) [4]. The new generation of faster, large-area single-photon imaging detectors consists of thin-film CsI UV-photocathodes, coupled to gas avalanche electron multipliers [5]. These devices are already successfully employed in RICH detectors, in some particle physics experiments, and are under construction in many others [6].

We discuss below the main factors governing the operation of this new family of gas avalanche photomultipliers and their principal properties. We summarize the recent progress made in UV and visible-range photocathodes, capable of operation under gas multiplication and suggest some preferable electron multipliers. Some applications are discussed.

2. General considerations

In gas avalanche photomultipliers with solid photocathodes (Fig. 1), photoelectrons are emitted into a gas. Depending on the type of electron multiplier coupled to the photocathode and on the electric field at the photocathode surface, they either drift to the multiplying electrode or experience a multiplication process at their emission location. In both cases, the surface photo-conversion, followed by surface emission, make these detectors very fast and insensitive to the radiation incidence angle, as

opposed to photon detectors where photo-ionization occurs within the volume of a photosensitive gas [7].

Unlike vacuum devices, these detectors can operate under high magnetic fields [8]. The operation under atmospheric gas-pressure permits constructing large area, thin, flat detectors of sizes limited mainly by the photocathode production technology. Highly integrated readout electronics [9], developed for particle physics applications, permits the conception of highly pixelized position sensitive photon detectors, capable of operation at high photon flux and under MHz frame rates.

The photon detection efficiency of these gas avalanche photomultipliers, over a given spectral range, depends on three factors: the photocathode quantum efficiency (QE), electron back-scattering from the photocathode into the gas [10] and the efficiency of detecting single electrons with the gas multiplier. The latter depends on the multiplier gain, its signal shape (which is multiplication-mechanism dependent) and on the readout electronics (integration time, noise).

The long-term stability principally depends on the photocathode, which may be degraded either by chemical reaction with gas impurities or by accumulated impact of photons and avalanche-originated ions. As discussed below, UV-photocathodes are generally chemically stable, while visible-range ones can be protected by coating them with thin films. Ion aging can be considerably reduced by a proper choice of the electron multiplier and the operation conditions.

3. Photocathodes

3.1.UV spectral range

The best known photocathode for the UV range is CsI. An extended review of its properties is given in ref.[5]. CsI has high absolute QE, of the order of 40% at 150nm, in a reflective mode; its red boundary cutoff is around 210nm, as shown in Fig. 2. Reflective CsI photocathodes, of typical thickness around 500 nm, are chemically stable; they can be exposed to ambient air for 30-60 min, without noticeable degradation of their emission properties. The chemical stability is of prime importance when installing such large area photocathodes within the photomultipliers, usually under inert gas flushing conditions.

CsI gaseous UV detectors were first applied as readout elements for Xenon-filled scintillation chambers [11]. Large-area CsI photon detectors have shown stable long-term behavior and adequate single-photon sensitivity under accelerator investigations [12]. Such detectors, of sizes exceeding a square meter, are under construction for the RICH detectors of the CERN-LHC-ALICE experiment [13]. Several other nuclear and particle physics experiments (GSI-HADES, CERN-COMPASS and others) have adopted this technique. It should be noted that the QE of 60 x 40 cm^2 large CsI photocathodes for ALICE, evaluated from experimental Cherenkov events, is about 20-30% lower for wavelengths below 180 nm, compared to the data shown in Fig.2 [13].

Two other UV-sensitive photocathodes, CsBr and chemical vapor deposited (CVD) diamond films, have recently been investigated. Their typical absolute QE distributions are also shown in Fig. 2.

CsBr photocathodes have not drawn any particular interest in the past, probably because of their spectral response which is limited to the far UV (cutoff at 0.1% QE around 190 nm)[14

photodetectors are requested, CsBr could be an excellent candidate. As shown in Fig.2, the QE of a CsBr film, which was subject to a post-evaporation thermal annealing under vacuum at 70 ^{0} C for about 6 hours, reaches values of the order of 30% at 150nm [14]. The quantum photoyield of our as-deposited CsBr films is inferior, with a cutoff at 175nm; it is similar to that previously published [15], as shown in Fig.3. Our recent investigations of reflective and transmissive CsBr photocathodes have shown that this material behaves rather similarly to CsI. Reflective photocathodes can be handled in ambient air for a few tens of minutes, with no apparent degradation and the surface aging of CsBr by intense photon flux and by ion impact also occurs after equivalent irradiation doses in both materials [14]. Charge multiplication in a CsBr-based parallel-plate gas avalanche detector was stable up to the investigated gains of the order of 10^4, though the surface resistivity of CsBr is apparently larger than that of CsI [16].

Recent investigations of the surface morphology of very thin (20-75nm) transmissive alkali halide films, clearly indicate their sensitivity to minute exposure to moisten gases, as shown in Fig.4 [17]. Particular care should therefore be taken while installing such transmissive photocathodes within the detectors.

CVD diamond films are also very interesting photosensitive materials [18]. Like mono-crystal diamonds, they have a wide energy band gap, of 5.47eV; they also have negative electron affinity (NEA), after surface hydrogenation [19]. Though having lower QE in the far-UV, compared to CsI and to CsBr, diamond photocathodes could find applications in detectors operating in a demanding environment, because of their known high chemical stability, radiation hardness and capability of operation under very high temperatures (hydrogen desorption occurs only above 800^{0}C). The QE curve shown in Fig.2 is for a diamond film whose surface was subject to hydrogen plasma etching. This establishes hydrogen surface termination, activating NEA, and was found to enhance the QE of CVD-prepared diamond films, by a factor of two[20]. Such surface treatment, yielding QE values of the order of 12% at 140 nm, is rather stable for short exposures to ambient air; long exposures, however, cause surface oxidation, resulting in positive electron affinity and therefore, loss of QE [20,21]. However, the photoemission properties could be recovered by repeated hydrogen-plasma etching. Other surface treatments, such as Cs-termination, could activate superior NEA on diamond films compared to that with hydrogen [22,23]; however the stability of Cs-terminated surfaces, under gas multiplication conditions, is still questionable.

3.2.Photocathodes for the visible range

The most important applications of gas avalanche photomultipliers, are, no-doubt in the visible spectral range. Here, alkali-antimonide photocathodes, in particular Cs_3Sb and K-Cs-Sb, are widely employed in vacuum-photomultipliers. These materials are extremely reactive to even minute amounts of impurities, e.g. oxygen and moisture. Therefore, some attempts at operating such photocathodes under gas multiplication [24,25], were not pursued.

A possible solution for avoiding the degradation of the reactive alkali-antimonide photocathodes is to coat them with thin protective films [26], allowing for the transport of photoelectrons, while preventing contact between the gas molecules and the photocathode. Intensive research of adequate protective materials for Cs_3Sb and

K-Cs-Sb photocathodes, coating conditions, electron transport properties, sensitivity to impurities, aging etc. have yielded very satisfactory results [27-30].

The coating film thickness is a compromise between the need for efficient photoelectron transmission (high QE) and the request for high stability under exposure to the counting gas. The best results were obtained with CsI and CsBr coating films [30], known for their good electron transport properties, reflected here by relatively small electron attenuation lengths (18 nm for CsI and CsBr, at 300 nm wavelength [31]).

Fig.5 shows typical distributions of the absolute QE, as function of wavelength, for bare K-Cs-Sb photocathodes and for ones coated with 25 and 30 nm thick CsI and CsBr films, respectively. The respective absolute QE values of these two coated photocathodes are of the order of 4% and 7% at 320 nm. These values represent about 4 to 6 times QE attenuation by the films, compared to the initial QE of the bare photocathode. These rather thick film coatings were chosen so as to protect the photocathodes against exposure to large amounts of oxygen. Indeed, Fig.6 shows the behavior of a bare and of two coated photocathodes, of different CsI film thickness, under exposure to oxygen. While the QE of the bare photocathode totally decays at 10^{-5} Torr of oxygen, the 20 nm thick film-coated one can withstand a 5 min exposure to 0.1 Torr, with a residual QE value of 10%. A 25-nm thick CsI film totally protects the photocathode, up to 150 Torr of oxygen, at the expense of further attenuation of the QE. However, this coating thickness permitted the storage of the photocathode at 150 Torr of oxygen, with practically no decay, for more than an hour [30]. Higher QE values are obtained with thinner coating films, which may still provide sufficient protection for operation of the photocathodes in ppm-purity level gases.

It should be stressed, though, that the alkali-halide coating-films do not provide sufficient protection against moisture; this is due to their hygroscopic nature, which tends to affect the surface continuity [17]. Other materials are being evaluated for protection against moisture. Some organic films were also studied for surface protection during production or transfer [32,33].

More results and details about visible-photocathode production and coating are given elsewhere [27-30,34].

4. Electron multipliers

As briefly discussed above, the type of electron multiplier coupled to the photocathode could play a decisive role. On one hand, it should provide high gas amplification for enhanced single-photon sensitivity; on the other hand, its operation mode should prevent an accelerated degradation of the photocathode and limit its exposure to avalanche-generated, photon- and ion-feedback effects. In addition, the photoelectron extraction efficiency strongly depends on the counting gas and on the electric field at the photocathode vicinity (electron back-scattering process). High electric fields enhance inelastic processes (excitation, ionization) on the account of elastic scattering, thus allowing for maximal electron extraction efficiencies, close to that in vacuum [10]. At electric fields above 10-20 $Vcm^{-1}Torr^{-1}$, gas multiplication starts in most gases; under these conditions, in addition to full extraction efficiency, the detector response is faster, due to the absence of electron drift and diffusion. However, a high field could have a serious drawback; the increased velocity of the back-drifting ions, impinging on the photocathode, may cause a faster degradation of its surface, by sputtering. The ion velocity can be reduced by a proper choice of the gas mixture [35].

The worst choice for an electron multiplier would be the parallel-plate avalanche chamber, where a high field is applied between the photocathode and an anode electrode. Here, all avalanche-induced ions sputter the photocathode at high velocity. Multi-step avalanche chambers, where the avalanche process occurs in successive parallel-grid elements, would be a better choice; it offers very high gain and only a fraction of the avalanche ions return to the photocathode [36]. Large-area CsI-based photon detectors generally employ MWPCs [6,13]. Here, the ions have high velocity at the vicinity of the anode wires, but they slow down at the photocathode region. Also, due to the field line distribution, only a fraction of the ions reach the

suffer from counting rate limitations; this could be a serious drawback in some applications, e.g. in medical imaging etc. Low-pressure operation of such multipliers is characterized, among others, by a fast ion clearance from the avalanche region and therefore by lack of space-charge effects [37]. It provides high gas gains and high rate capability, but at the expense of shorter photocathode lifetime due to more energetic ion sputtering [36].

Modern micro-pattern gas electron multipliers [38] could provide an adequate
                          39   40   41], and other compact
multiplying electrodes have been employed in combination with CsI photocathodes. They consist of precise and dense anode and cathode patterns (strips, dots etc.), 50-200 micron distant, deposited on insulating substrates. Due to the particular electric field geometry, a large fraction of the avalanche ions, created at the vicinity of the anode patterns, are collected at neighboring cathode electrodes, rather than returning to the photocathode (Fig. 1). This rapid ion clearance from the avalanche region results in high counting rate capability and in fast electrical pulse buildup. It has been demonstrated that the low-pressure operation of such micro-pattern devices provides, in addition, very high gains and fast response [39,41], as shown in Fig.7.
                          42   -   43] and
                          44] multipliers, where the avalanche develops over
very small distances (50-100 microns).

The GEM particularly, could suit our application, due to very special electrode geometry. This simple multiplier consists of a compact array of small apertures in a metal-coated, 50-micron thick, Kapton foil. The apertures, of 30-100 micron in diameter, are typically spaced by 150-200 microns. A potential difference of a few hundred volts across the GEM foil leads to avalanche formation within the apertures, reaching amplification factors above 1000 in a single element, both at atmospheric [45] and low [46,47] gas pressures. Very high gains, exceeding 10^5, and stable operation have been reached in GEM-based photomultipliers, by cascading a GEM with another multiplying element [46,47] (see Fig.8) or by cascading several GEMs operating even with noble gas mixtures [35,48] (see Fig.9).

The GEM inserted in a gas avalanche photodetector, between the photocathode and the following multiplication elements, will play a multiple role:

- It would transmit photoelectrons into the multipliers, while screening the photocathode from avalanche-induced feedback photons, as demonstrated in ref.46 (Fig.10).
- In some electric field configurations, the GEM would block a fraction of the back-drifting ions.
- Some gain on the GEM will permit reducing the gain on the following multiplication elements, leading to more stable operation. It will allow for higher total gain and therefore higher sensitivity to single photons.

- The almost complete elimination of photon feedback effects in multi-GEM structures, permits, for the first time, reaching very high gains (> 10^5) in noble gas mixtures [49,35,48]. This should permit the operation with sensitive alkali antimonide visible photocathodes.
- The thin GEM electrode permits very fast avalanche development, leading to fast signals [35,47] and therefore to good time resolution.
- The deposition of a photocathode on top of the GEM surface (Fig.11) [46] should permit an operation free of photon feedback effects.

5. Conclusions

Gas avalanche photomultipliers, with their numerous advantages, have become interesting potential tools for high resolution, fast photon imaging tasks in numerous applications. In the UV range, very large area (square meters) CsI-based gaseous imaging devices are under construction for RICH detectors. CsBr and CVD diamond photocathodes have interesting properties in the far UV (solar-blind) range. The quantum efficiency of the diamond films can be enhanced by surface modifications, but most probably at the expense of chemical stability.

Ways have been paved towards imaging of visible light with gaseous photomultipliers. Conditions were found for protecting alkali-antimonide photocathodes against oxygen, with 25-30 nm thick alkali-halide (CsI, CsBr) films. Coated K-Cs-Sb photocathodes, having QE values of 5-6% in the 300-350nm spectral range, can withstand long exposures to over 100 Torr of Oxygen. However good protection against moisture is more problematic, due to the hygroscopic nature of alkali-halide films. Other coating films, among them organic materials, are investigated for possible protection against moisture. Higher QE values were reached with thinner protective films, which would suit the operation of these photomultipliers in high purity gases.

Alkali-halides and alkali-halide-coated visible photocathodes undergo moderate aging under intense photon illumination and gas multiplication. In our estimation, this should not prevent their use, even at extreme photon imaging conditions.

The damage induced by avalanche ions can be largely reduced by employing modern micro-pattern electron multipliers. In devices having electrode patterns printed on insulating substrates (MSGC, MDOT, MGC) or in others, where multiplication occurs within tiny apertures (GEM), or within fine-grid structures (MICROMEGAS, micro-CAT), one can find operation conditions for preventing most of the avalanche ions from reaching the photocathode. Of particular interest is the recently proposed multi-GEM multiplier.

Besides the present application of UV-photon imaging in Ring Imaging Cherenkov (RICH) Detectors, gas avalanche photomultipliers have a broad spectrum of potential applications. These fast, large area imaging detectors, capable of operation at repetition rates superior to a MHz/mm^2 and under high magnetic fields, could be employed for photon recording from large scintillator and scintillating fiber arrays. The latter have numerous applications in particle and nuclear physics and in medical diagnostics apparatus. An application of visible-light gas avalanche photomultipliers for digital mammography is in progress, within a European Union project [50].

Acknowledgements

References

1. R. De Salvo et al., Nucl. Instr. and Meth. A 315 (1992) 375.
2. C. Joram, Proc. of the Sixsth Int. Conf. on Advanced Technology and Particle Physics, Como, Italy, October 1998, in press.
3. J.   371 (1996) 33 and references therein.
4. J. Seguinot and T. Ypsilantis, Nucl. Instr. and Meth. A 343 (1994) 30 and references therein.
5. A. Breskin, Nucl. Instr. and Meth. A 371 (1996) 116 and references therein.
6. F. Piuz, Nucl. Instr. and Meth. A 371 (1996) 96 and references therein.
7. A. Breskin, Nucl. Phys. B (Proc. Suppl.) 44 (1995) 351.
8. F. Piuz et al., Nucl. Instr. and Meth. A 433 (1999) 178.
9. P. Weilhammer, Nucl. Instr. and Meth. A 433 (1999) 413.
10. A. Di Mauro et al., Nucl. Instr. and Meth. A 371 (1996) 137 and references therein.
11. V. Dangendorf et al., Nucl. Instr. and Meth. A 289 (1990) 322.
12. F. Piuz et al., Nucl. Instr. and Meth. A 433 (1999) 222.
13. A. Di Mauro et al., Nucl. Instr. and Meth. A 433 (1999) 190.
14. B. K. Singh et al., On the properties of CsBr UV-photocathodes. In preparation.
15. E. A. Taft and H. R. Philipp, J. Chem. Solids 3 (1957) 1.
16. J.   387 (1997) 154.
17. T. Boutboul et al., On the surface morphology of thin alkali-halide photocathode films. Nucl. Instr. and Meth. A, in press.
18. A. Breskin et al., Appl. Phys. Lett. 70 (1997) 3446.
19. J. Ristein et al., Diamond and Relat. Mater. 7 (1998) 626.
20. A. Laikhtman et al., Appl. Phys. Lett. 84 (1998) 1443.
21. A. Laikhtman et al., Diamond and Relat. Mater. 8 (1999) 725.
22. G. T. Mearini et al., Appl. Phys. Lett. 66 (1995) 242.
23. M. Niigaki et al., Jap. J. Appl. Phys. 37 (1998) L1531.
24. G. Charpak et al., IEEE Trans. Nucl. Sci. 30 (1983) 134.
25. J. Edmends et al., Nucl. Instr. and Meth. A 273 (1988) 145.
26. V. Peskov et al. Nucl. Instr. and Meth. A 348 (1994) 269 and A 353 (1994) 184.
27. A. Breskin et al. Appl. Phys. Lett. 69 (1996) 1008.
28. A. Buzulutskov et al., Nucl. Instr. and Meth. A 400 (1997) 173.
29. E. Shefer et al., Nucl. Instr. and Meth. A 419 (1998) 612.
30. E. Shefer et al. Nucl. Instr. and Meth. A 433 (1999) 502.

31. E. Shefer et al., Photoelectron transport through CsI, CsBr and NaI coating films. In preparation.
32. A. Breskin et al., Nucl. Instr. and Meth. A 413 (1998) 275.
33.
    World Scientific Publishing (1999) pg. 195.
34. E. Shefer et al., Nucl. Instr. and Meth. A 411 (1998) 383.
35. A. Buzulutskov et al., The GEM photomultiplier operated with noble gas mixtures. Nucl. Instr. and Meth. A, in press.
36. V. Dangendorf et al., Nucl. Instr. and Meth. A 308 (1991) 519 and references therein.
37. A. Breskin, Nucl. Instr. and Meth. 196 (1982) 11.
38. F. Sauli, Nucl. Instr. and Meth. A 419 (1998) 189.
39. A. Breskin et al., Nucl. Instr. and Meth. A 345 (1994) 205.
40. F. Angelini et al. Nucl. Instr. and Meth. A 362 (1995) 273.
41. A. Breskin et al., Nucl. Instr. and Meth. A 394 (1997) 21.
42. Y. Giomataris, Nucl. Instr. and Meth. A 419 (1998) 239.
43. A. Sarvestani et al. Nucl. Instr. and Meth. A 419 (1998) 444.
44. F. Sauli, Nucl. Instr. and Meth. A386 (1997) 531.
45. J. Benlloch et al., Nucl. Instr. and Meth. A 419 (1998) 410.
46. R. Chechik et al., Nucl. Instr. and Meth. A 419 (1998) 423.
47. G. Garty et al., Nucl. Instr. and Meth. A 433 (1999) 476.
48. A. Buzulutskov et al. Further studies of the GEM photomultiplier. Proc. of BEAUNE99, to be published in Nucl. Instr. and Meth. A.
49. A. Bressan et al., Nucl. Instr. and Meth. A423 (1999) 119.
50. The MICADO project, European Union Contract No.IN205891.

Figure Captions

Figure 1: The principle of the gas avalanche photomultiplier. A photon-induced electron is emitted from a solid photocathode into the gas. Avalanche multiplication takes place in the electron multiplier, close to an anode of a micropattern device. In this configuration, most avalanche-induced ions are collected on the neighboring cathodes and some drift to the photocathode.

Figure 2: Typical quantum efficiency plots (in vacuum) of annealed CsI [5], CsBr [14], and of hydrogen-terminated CVD-diamond [20] photocathodes.

Figure 3: Absolute quantum efficiency plots (in vacuum) of a 500 nm thick CsBr photocathode, as evaporated and after an annealing of 3 and 6 hours at 70^0C. Data of Taft and Philipp [15] is shown for comparison.

Figure 4: SEM views of thin alkali-halide photocathodes deposited on CaF_2/Cr substrates. a) a 20 nm thick CsI film, as-evaporated; b) same as (a) after exposure to air for 9 minutes; c) a 75 nm thick CsBr film, as evaporated; d) same as (c) after exposure to Argon at 80% humidity for 1 minute. The full scale, in all cases is 5μm.

Figure 5: Typical absolute quantum efficiency spectra of K-Cs-Sb photocathodes, bare and coated with 300   250

Figure 6: The evolution of the absolute quantum efficiency of K-Cs-Sb photocathodes exposed to oxygen. Shown are the results of bare and coated photocathodes with 200   and 250   thick CsI films, as a function of the residual oxygen pressure at 312nm. Each data point represents 5 minutes of exposure to oxygen followed by quantum efficiency measurement in vacuum.

Figure 7: Fast single electron pulses obtained from a) a Microdot gas avalanche chamber operated in 60 Torr of C_3H_8; b) A multiwire proportional chamber (MWPC) operated in 40 Torr of i-C_4H_{10} and c) the same MWPC coupled to a GEM (at gain 250). All pulses measured with the same fast current amplifier.

Figure 8: A gas avalanche photomultiplier comprising of a GEM electron preamplifier, inserted between the photocathode and the electron multiplier (here a MWPC). The GEM enables reducing the gain on the MWPC and screens the photocathode from photon feedback.

Figure 9: A multi-GEM photomultiplier consisting of a cascade of GEMs coupled to a photocathode. Each GEM operates at a low gain, resulting in a high total gain. The resulting avalanche induced pulses can be recorded on a printed circuit board, without any additional multiplication. The GEM elements screen the photocathode from photon-feedback and reduce ion-feedback effects.

Figure 10: Photon-feedback in 40 Torr methane: a) A MWPC coupled to a CsI photocathode; has an intense photon-feedback, gain <10^5; b) a MWPC+GEM (see figure 9), a reduced photon feedback and gain >5×10^6

Figure 11: A photon-feedback blind detector: photons are converted on a reflective photocathode deposited on a GEM. The photoelectron is focussed into the GEM holes, is preamplified and further amplified in the MWPC. Avalanche-induced photons cannot reach the photocathode.
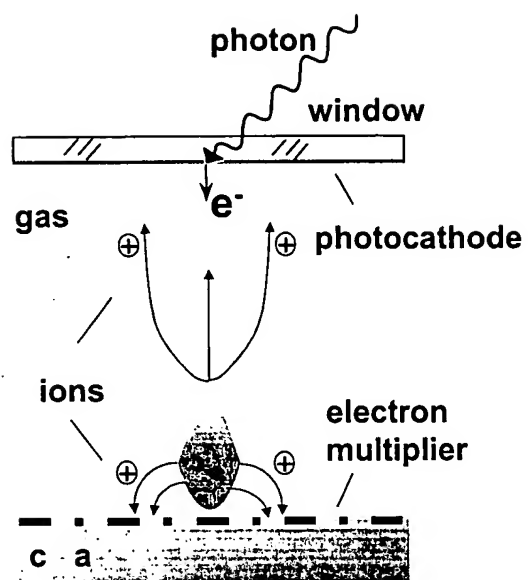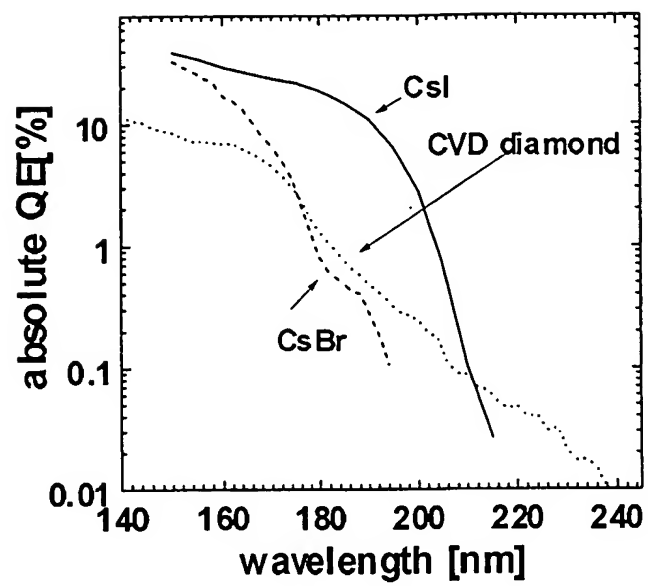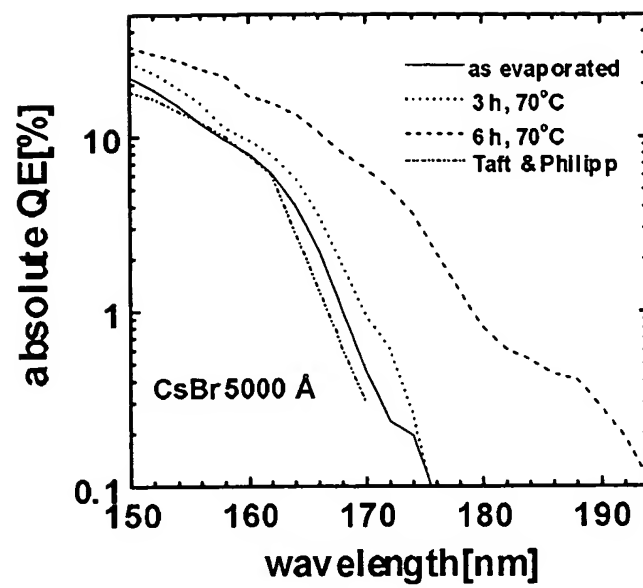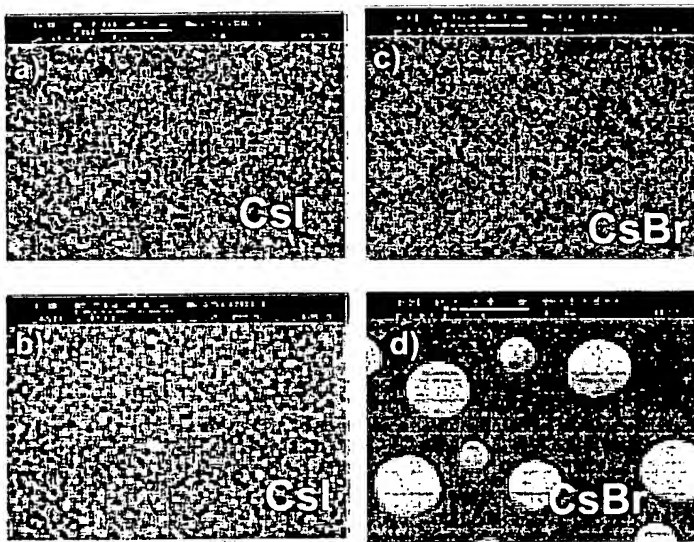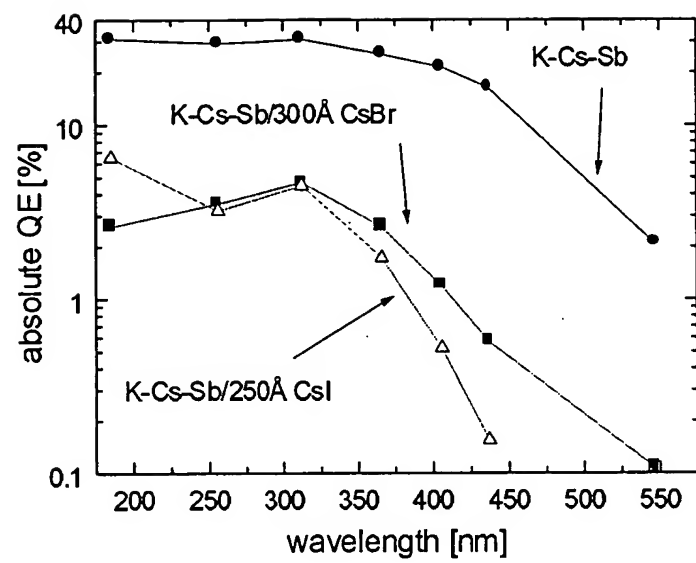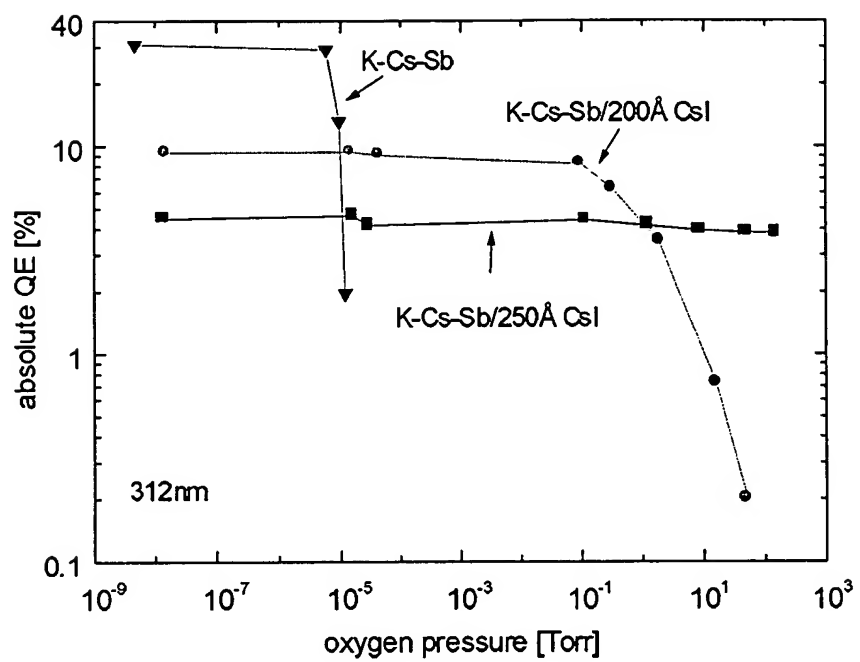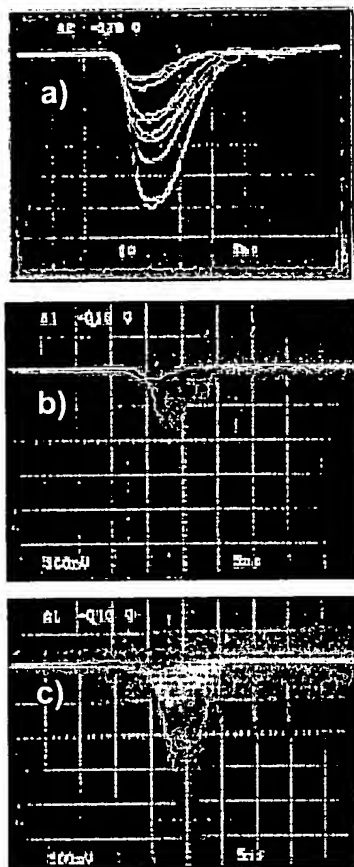
Figure 1

Figure 2

Figure 3

Figure 4
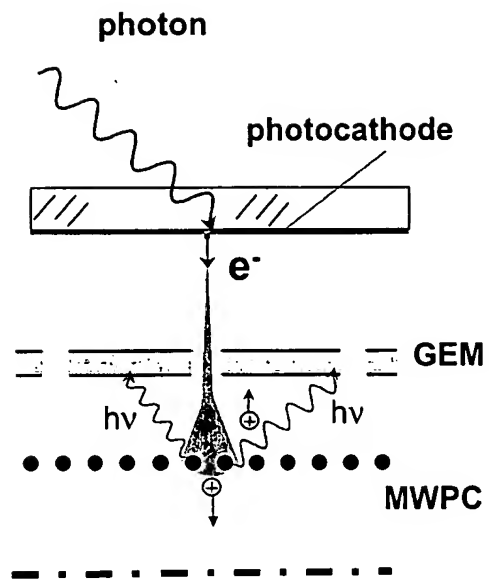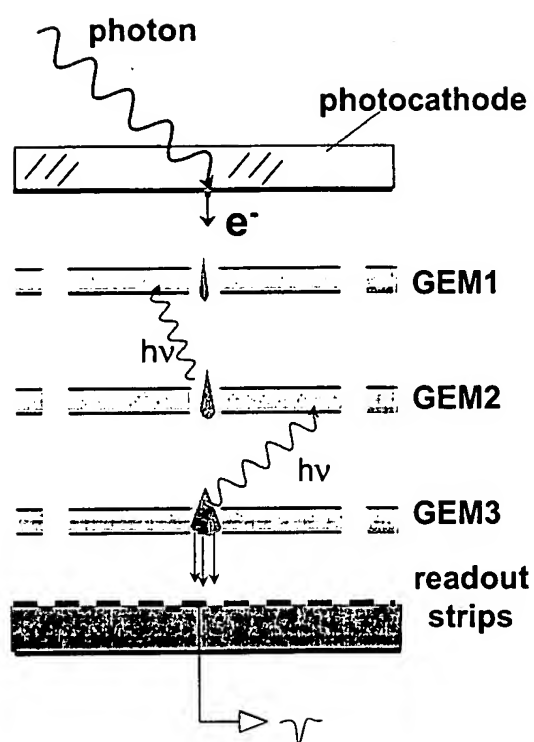
Figure 5

Figure 6

Figure 7

photon

photocathode

e⁻

GEM

hv   hv

MWPC

Figure 8

Figure 9

Figure 10

Figure 11